CrossMark

ER Stress Induced by Tunicamycin Triggers α-Synuclein Oligomerization, Dopaminergic Neurons Death and Locomotor Impairment: a New Model of Parkinson's Disease

Valentín Cóppola-Segovia[1] · Clarissa Cavarsan[1] · Flavia G Maia[1] · Anete C Ferraz[2] ·
Lia S Nakao[1] · Marcelo MS Lima[2] · Silvio M Zanata[1]

Abstract Parkinson's disease (PD) is a neurodegenerative disorder characterized by progressive death of dopaminergic neurons of the substantia nigra pars compacta (SNpc), leading to the major clinical abnormalities that characterize this disease. Although PD's etiology is unknown, α-synuclein aggregation plays a pivotal role in PD pathogenesis, which could be associated to some pathological processes such as oxidative stress, endoplasmic reticulum (ER) stress, impaired protein degradation, and mitochondrial dysfunction. Increasing experimental evidence indicates that ER stress is involved in PD, however most of the described results employed cultured cell lines and genetically modified animal models. In this study, we developed a new ER stress rat model employing the well-known ER stressor tunicamycin (Tm). To evaluate if ER stress was able to induce PD features, we performed an intranigral injection of Tm (0.1 μg/cerebral hemisphere) and animals (male Wistar rats) were analyzed 7 days post injection. The classical 6-OHDA neurotoxin model (1 μg/cerebral hemisphere) was used as an established positive control for PD. We show that Tm injection induced locomotor impairment, dopaminergic neurons death, and activation of astroglia. In addition, we observed an extensive α-synuclein oligomerization in SNpc of Tm-injected animals when compared with DMSO-injected controls. Finally, both Tm and 6-OHDA treated animals presented increased levels of ER stress markers. Taken together, these findings show for the first time that the ER stressor Tm recapitulates some of the phenotypic characteristics observed in rodent models of PD, reinforcing the concept that ER stress could be an important contributor to the pathophysiology of PD. Therefore, we propose the intranigral Tm injection as a new ER stress-based model for the study of PD in vivo.

Keywords Parkinson's disease · ER-stress · Tunicamycin · α-Synuclein oligomerization

Introduction

Parkinson's disease (PD) is the second most common neurodegenerative disorder, caused by selective degeneration of dopaminergic neurons of the *Substantia Nigra pars compacta* (SNpc) [1, 2]. Dopaminergic deficit results in motor disabilities, such as rest tremor, bradykinesia, rigidity of movement, and postural instability [3]. Despite the existence of specific genetic causes, PD is primarily a sporadic disorder. Although the etiology of PD remains unknown, environmental or genetic factors might contribute to the pathogenesis of PD, leading to an increase of oxidative stress, endoplasmic reticulum (ER) stress, and impairing mitochondrial function [4–7]. Besides dopaminergic neuronal death, neuropathological hallmarks of PD include glial reactivity, inflammation, and intracellular proteinaceous inclusions called Lewy bodies (LB), which are mainly constituted by α-synuclein aggregates [4, 6].

Genetic and transgenic animal models support the idea that the accumulation of fibrillar α-synuclein plays a relevant role in the pathogenesis of PD [8]. However, mounting evidence [9] indicates that soluble pre-aggregate oligomers are responsible for neurodegeneration, having aggregates a clearance

✉ Silvio M Zanata
smzanata@ufpr.br

1   Laboratory of Neurobiology and Redox Pathology, Department of Basic Pathology, Setor de Ciências Biológicas, Universidade Federal do Paraná, Av. Francisco H. dos Santos, s/n, Curitiba 81531-980, Paraná, Brazil

2   Department of Physiology, Universidade Federal do Paraná, Curitiba, Brazil

function since they could immobilize the oligomeric α-synuclein, avoiding its toxic availability.

Abnormal forms of α-synuclein and oligomers lead to cellular homeostasis imbalance that includes alterations of calcium signaling [10, 11], mitochondrial dysfunction [12], oxidative and nitrosative damage [13], changes in cytoskeletal integrity [14], and neuroinflammation [15].

Despite the ubiquitous presence of α-synuclein in LB [16] and its relevance in the development of PD [8], the molecular mechanism mediating the neurotoxicity of α-synuclein remains unclear and still in debate [17].

Cytosolic and membrane bound levels of α-synuclein are regulated by their synthesis, degradation, and secretion rates and a proteostasis imbalance has been shown to be involved in aggregates formation. The ubiquitin-proteasomal system dysfunction contributes to inclusions formation and toxicity [18, 19]. Furthermore, post-translationally modified α-synuclein is impaired to be degraded by the autophagy-lysosome pathway [20], indicating that disturbance of the two main routes responsible for protein degradation triggers α-synuclein accumulation in the cell, leading to ER stress.

Approximately, one third of cellular proteins are synthesized in the ER where they are folded and undergo post-translational modifications, and transit to membrane compartments or are secreted [21]. However, under certain conditions of cellular stress, protein folding is altered, and misfolded substrates accumulate in the lumen of ER triggering an adaptive signaling pathway called unfolded protein response (UPR) [21, 22]. This mechanism is regulated by the ER resident chaperone glucose-regulated protein-78 (GRP78) that mediates the activation of three major stress sensors: protein kinase RNA-like ER kinase (PERK), inositol requiring enzyme-1 (IRE1), and activating transcription factor-6 (ATF6) [21]. The initial role of UPR is to restore homeostasis and alleviate ER stress through attenuation of protein translation, increase folding capacity, ER membrane expansion and activation of ER-associated degradation (ERAD pathway) [21–24].

Endoplasmic reticulum (ER) stress has recently acquired great attention in the field of neurodegenerative diseases [25, 26], particularly with respect to PD [27]. In fact, post-mortem analysis has demonstrated that substantia nigra of PD cases present activation of the PERK pathway, which is correlated with increased levels of α-synuclein in dopaminergic neurons [28]. Additionally, the C/EBP-homologous protein (CHOP), a downstream member of the PERK pathway [21], is up-regulated in the 6-OHDA neurotoxin-induced cell death both in vitro [29] and in vivo [30], corroborating the findings that CHOP knockout mice dopaminergic neurons are protected from cell death after 6-OHDA challenge [31]. Besides PERK, the IRE1 and ATF6 branches of the UPR have also been implicated in PD [27], however most of the experimental data were obtained employing cultured cell lines or neurons

[32, 33] and transgenic animals [34, 35]. These data collectively suggest that the UPR is activated in PD and that UPR activation is closely associated with the accumulation and aggregation of α-synuclein and dopaminergic cell death.

Because increasing evidences point to the pivotal role the ER stress and UPR in PD and there is lacking of in vivo ER stress models that use only non-genetically manipulated animals, we developed a new ER stress rodent model employing an intranigral injection of the well-known ER stressor tunicamycin (Tm) [36]. First, we found that Tm injection induced locomotor impairment, dopaminergic neurons death, and activation of astroglia. In addition, we observed an extensive α-synuclein oligomerization in SNpc of Tm-injected animals when compared with control. In this context, the classical 6-OHDA neurotoxin-based model was employed as an established positive control for PD [31, 37, 38]. Finally, animals challenged with Tm presented increased levels of ER stress markers, indicating that the UPR signaling was activated in this new animal model, which in turn recapitulates several features of PD. Therefore, we propose the intranigral Tm injection as a new ER stress-based model for the study of PD in vivo.

Materials and Methods

Animals

Experimental procedures were performed in accordance with the Ethics Committee for Research on Animals UFPR (protocol #778). Fifty-eight adult male Wistar rats 9 weeks old, weighing 280–320 g at the beginning of the experiments were used. Animals were housed in groups of five, in polypropylene cages and maintained under standard conditions of temperature (22 ± 2 °C) and illumination (12/12 h light/dark cycle). The animals had free access to water and food throughout the experiments.

Surgical Procedures

Animals were anesthetized using ketamine/xilazine (100 mg/kg; 20 mg/kg; Syntec do Brasil Ltda, Brazil) intraperitoneally, and placed in a stereotaxic frame. The following coordinates were used to the bilateral injury, bregma as a reference: SNpc (AP) = −5.3 mm, (ML) = ± 2.1 mm e (DV) = −7.8 mm (Paxinos and Watson, 2005). 5 mg/ml stock solution of Tm (Sigma) was prepared in dimethylsulfoxide (DMSO) (Sigma). Needles were guided to the region of interest for a bilateral infusion of 0.5 μL of Tm prepared at a final concentration of 0.2 mg/mL diluted in PBS (1:25 dilution from the stock solution). As a positive control of the lesion, 1 μL of the neurotoxin 6-hydroxydopamine (6-OHDA) (Sigma) dissolved in PBS at a final concentration of 1 mg/mL, supplemented with

0.2 % of ascorbic acid was injected. Also, the sham procedure (control group) received 1 μL of the vehicle (PBS:DMSO, 1:25). The infusions were performed with an electronic pump (Harvard Apparatus, Holliston, MA, USA) at a flow rate of 0.33 μL/min. After each infusion the needle was kept in the injection site for additional 2 min to avoid reflux.

Footprint Analysis

One week after surgery, animals were evaluated for motor coordination and balance [39]. A 100-cm long, 10-cm wide runway (with 35-cm high walls) was used for footprint test. Before collecting footprints, each animal was able to explore the runway for 5 min. After recognition, animal's paws were painted with water-based nontoxic paint (using different color for hindpaws and forepaws), and each animal was immediately placed at one end of the runway previously covered with a strip of paper as template. Data were collected when the animal was able to walk without interruption giving at least four steps in a straight line for each paw (initiation and finishing of the run were ignored) [40, 41]. The paper was removed for analysis and fore and hind step parameters were analyzed according to an established methodology [40].

Western Blot Analysis

To determine ER stress within the *substantia nigra* (SN), 7 days after injection with 6-OHDA or Tm, animals were decapitated, their brains were rapidly ice-removed and SN was dissected. Until processed for analysis, tissues were stored at −80 °C in lysis buffer containing 50 mM NaCl, 50 mM Hepes, 2 mM EDTA, 1 % Triton X-100, 1 mM PMSF, 1 mM sodium orthovanadate, and complete protease inhibitor mixture EDTA-free (Roche). Samples were manually homogenized on ice using a micropestle (Eppendorf). After centrifugation (10 min 12,000×g at 4 °C), supernatant was collected. Protein concentration was determined by the Bradford method (Bio-Rad, Germany). Samples were subjected to SDS-PAGE and proteins transferred to a nitrocellulose membrane (GE Healthcare). The membranes were then blocked in 5 % slime milk or BSA in TBS-T (blocking solution) for 1 h at room temperature and incubated 16 h with the desired antibody diluted in blocking solution. Employed antibodies were: mouse monoclonal anti-β-actin (A5441, Sigma), anti-α-synuclein (610787 BD), anti-CHOP (MA1-250, Thermo Scientific), anti-KDEL (ADI-SPA-827, Enzo Life Science) and anti-GAPDH (#2118, Cell Signaling). After primary antibody incubation, membranes were extensively washed with TBS-T and incubated with HRP-conjugated secondary antibody (Sigma) in blocking solution for 1 h at room temperature. Finally, membranes were washed again and immune complexes were detected using the ECL chemiluminescent detection system (GE Healthcare Life Sciences, Brazil). The protein levels were quantified by densitometry using ImageJ v1.47 software (National Institutes of Health, USA).

Imunohistochemistry

Animals were deeply anesthetized using ketamine/xilazine (100 mg/kg/20 mg/kg), and transcardially perfused with PBS, followed by 4 % paraformaldehyde in PBS (pH 7.2) at a constant flow of 1 mL/min. Fixed brains were quickly removed and post-fixed by immersion in 4 % paraformaldehyde for 24 h. The brains were immersed in 30 % sucrose solution for cryoprotection, and stored at −80 °C until cryostat sectioning (Leica Lm 1850, Germany). Brains were sliced into 30-μm coronal sections (Bregma: −5.16 to −5.40) and stored in anti freezing solution (30 % ethylene glycol, 30 % sucrose in PBS) at −20 °C. Free-floating sections were permeabilized for 15 min at room temperature with 0.1 % Triton X-100 in PBS, treated with 0.3 % H_2O_2 for 20 min, washed three times with PBS followed by blocking with 5 % BSA for 30 min and incubation overnight with mouse anti-tyrosine hydroxylase (TH) (T2928, Sigma) or rabbit anti-GFAP (Z0334, DAKO) antibody at 4 °C. Antibodies were detected using HRP immunostaining kit (Diagnostic Biosystems). Tissues were dehydrated in aqueous graded ethanol solutions from 70 to 100 % and then immersed twice in xylene and mounted with Entellan New (Merck).

Statistical Analysis

Differences between the groups were analyzed by one-way analysis of variance (ANOVA) followed by Tukey post hoc tests. Values are expressed as mean ± standard error of mean (SEM). The level of significance was set at $P \leq 0.05$.

Results

We first examined whether the ER stressor Tm could induce locomotor disturbances in animals subjected to direct drug delivery into SNpc, as typically observed in other well-established animal model of PD [31, 37, 38]. Seven days after challenging rats with a single bilateral injection of Tm or 6-OHDA, footprint test was performed to assess locomotor performance. Quantitative analyzes showed absence of statistical differences in the stride length of hindpaw and forepaw between groups (Fig. 1a). While the stance width of the forepaws did not show difference between groups, hind paws instead was significantly broader in Tm- and 6-OHDA-injected ($P < 0.01$) animals [$F_{[2, 24]}$= 7.986; $P = 0.0022$] (Fig. 1b) in comparison with the control group.
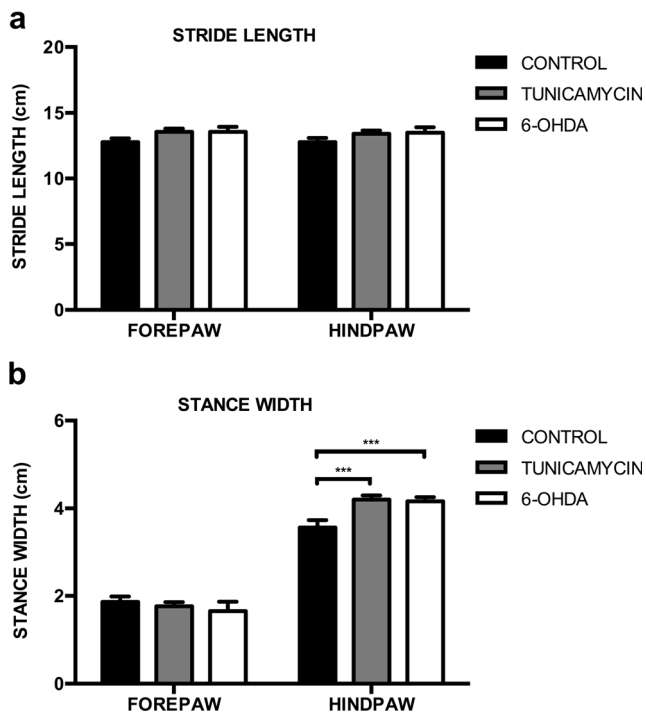
Fig. 1 Footprints reveal gait abnormalities in animals challenged by Tm. **a** Stride lengths and **b** stride width for hind- and fore-paws measured with the footprint test. Data is represented as the mean ± SEM (*CONTROL* $n = 10$; *TUNICAMYCIN* $n = 8$; *6-OHDA* $n = 9$), asterisks indicate statistical differences (***) $p \leq 0.01$ compared with the control group

After locomotor assessment, animals were sacrificed and brains evaluated for dopaminergic neuronal loss by TH immunostaining at SNpc level. Figure 2 shows representative images of coronal midbrain sections of TH-immunoreactive neurons for control (sham), Tm and 6-OHDA (positive control) groups (Fig. 2a–c, respectively). Quantification (Fig. 2d) of TH-immunopositive neurons in SNpc showed a decrease of 25 % ($P < 0.05$) and 22 % ($P < 0.05$) for Tm and 6-OHDA groups respectively, when compared to the control group [F [2, 10]= 6.497; $P = 0.0156$].

As a hallmark for neurodegeneration, reactive astrogliosis was examined with antibody against GFAP (Fig. 3) [42]. GFAP immunohistochemistry of coronal midbrain section from Tm and 6-OHDA injected animals showed ~2.6 ($P < 0.0001$) and ~2.9 increasing fold ($P < 0.0001$) of GFAP$^+$ astrocytes when compared to control animals [F [2, 10]= 33.11; $P < 0.0001$], respectively (Fig. 3d). In addition, astrocytes from Tm and 6-OHDA animals presented morphological changes [42] such as cellular hypertrophy and up-regulated expression of GFAP (Fig. 3b'–c', respectively), when compared to control animals (Fig. 3a').

Based on previous studies that associate ER stress to protein misfolding [43–45], and because α-synuclein misfolding is a hallmark of PD [28, 46], we analyzed α-synuclein expression and its oligomeric status by western blot after Tm treatment. Interestingly, analysis of α-synuclein expression

showed no difference in monomeric α-synuclein levels between groups ($P = 0.4336$) (Fig. 4a, mid panel and Fig. 4b). However, Tm injected animals showed increased high molecular weight forms of α-synuclein ($P < 0.01$) [F [2, 11]= 9.633; $P = 0.0038$] (Fig. 4a, upper panel and Fig. 4c) indicating that the ER stressor Tm can induce in vivo one of the molecular features of PD.

As a major consequence of ER stress, UPR activation triggers repression of translation and up-regulation of ER-resident chaperones after accumulation of misfolded proteins [47, 48]. In order to measure the intensity of ER stress observed after injury, ER-resident chaperones were evaluated by western blot with anti-KDEL tetrapeptide signal (Fig. 5a). Quantification of ER-resident chaperone levels presented an ~2.9 and ~2.5-fold increase for GRP78 ($P < 0.05$) [F [2, 12]= 6.411; $P = 0.0128$] (Fig. 5c), and ~9.4 ($P < 0.001$) and ~7.5-fold ($P < 0.05$) increase for GRP94 for Tm- and 6-OHDA-treated animals, respectively [F [2, 12]= 8.695; $P = 0.0046$], when compared to control animals (Fig. 5b), indicating that both Tm and 6-OHDA challenges increase ER-resident chaperones.

Upon ER stress, GRP78/GRP94 luminal chaperones dissociate from ER-resident membrane proteins, which transmit downstream UPR activation signals to the cytoplasm [21, 49]. To clarify if the dopaminergic lesion (Fig. 2) was accompanied by PERK pathway signaling modulation, we performed western blot analysis of CHOP in SN samples (Fig. 6a). Despite the PERK-CHOP pathway has been described as the major UPR-associated pro-apoptotic branch [21, 50] we only observed a tendency to increase levels of CHOP in Tm group (Fig. 6b, $P < 0.10$) when compared to the control group, suggesting that other UPR pathway could be involved in neuronal cell death. Confirming previously described results [30], animals presented increased expression of CHOP under 6-OHDA treatment (Fig. 6b, $P < 0.05$) [F [2, 15]= 4.649; $P = 0.0268$], reinforcing the role of ER stress in these established animal PD model.

Discussion

There are several factors that may be associated with the genesis of neurodegenerative diseases. Genetic causes, inflammation, ATP generation deficiency, increases in ROS production, mitochondrial dysfunction, ER stress and protein degradation pathways have been associated with neurodegenerative progression in PD both in animal models and humans [25, 51]. In the present study, we propose a novel in vivo model to the study of Parkinsonism induced by ER stress.

Increased expression of ER-resident chaperones, such as GRP78 and GRP94 is thought to be a response against ER stress, in order to increase protein-folding capacity and alleviate stress conditions (21, 48, 49). In view of that, previous in vitro studies demonstrated that 6-OHDA, 1-methyl-4-

CONTROL TUNICAMYCIN 6-OHDA
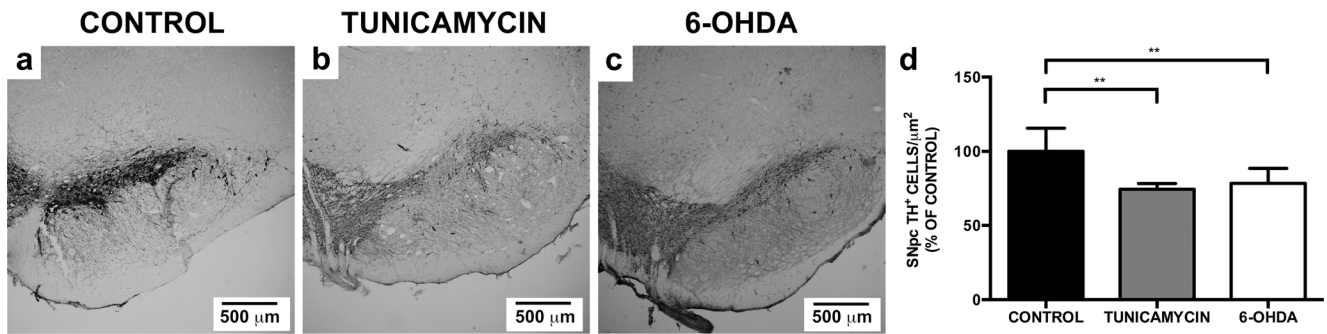
Fig. 2 Dopaminergic cell loss induced by Tm. Representative microphotographs showing TH-immunoreactivity of midbrain coronal sections of **a** Control, **b** Tm and **c** 6-OHDA injected animals 7 days post-lesion. **d** Quantification of TH-positive cell number in SNpc. Data are represented as the mean ± SEM (*CONTROL n = 5; TUNICAMYCIN n = 4; 6-OHDA n = 4*). Asterisks indicate statistical differences (**) $p \leq 0.05$

phenylpyridinium (MPP$^+$) and rotenone induce activation of ER-stress pathways and promote cellular death in neuronal cultures [29, 32], indicating that known drugs that induce PD also induce ER stress. 6-OHDA is a classical neurotoxin that leads to PD by mechanisms of selective dopaminergic neuronal death by H_2O_2 and quinone generation [52]. The fact that cultured sympathetic neurons from PERK$^{-/-}$ knockout mice were more susceptible to die than wild-type neurons when exposed to 6-OHDA indicates the importance of ER stress in PD pathophysiology [32] and suggests that other UPR pathways may contribute to induce cell death. Moreover, mice with 6-OHDA intracerebroventricularly injected showed GRP78 increase in striatum [30]. Our data extend these findings as demonstrated by the increase in both GRP78 and GPR94 expression levels after 6-OHDA

treatment and reinforce the role of the ER stress in the 6-OHDA neurotoxicity rat model. In addition, the ER stressor employed in this study, Tm, also increased levels of GRP78 and GRP94 7 days after lesion (Fig. 5a–c), as similarly observed for GRP78 after ventricular administration of Tm and thapsigargin [53]. Although CHOP induction is classically associated to PERK-eIF2α-ATF4 pathway, CHOP levels of Tm injected animals showed no statistical difference when compared to the control group (Fig. 6), suggesting that increased levels of GRP78/GRP94 after lesion (Fig. 5a–c) could be related to other ER-stress pathways, like ATF6 or IRE1 [54–57]. Taken together, these results suggest that ER stress is a common event in these models of PD.

Under ER stress conditions, activation of PERK pathway leads to eIF2α phosphorylation, activating transcription factor

CONTROL TUNICAMYCIN 6-OHDA
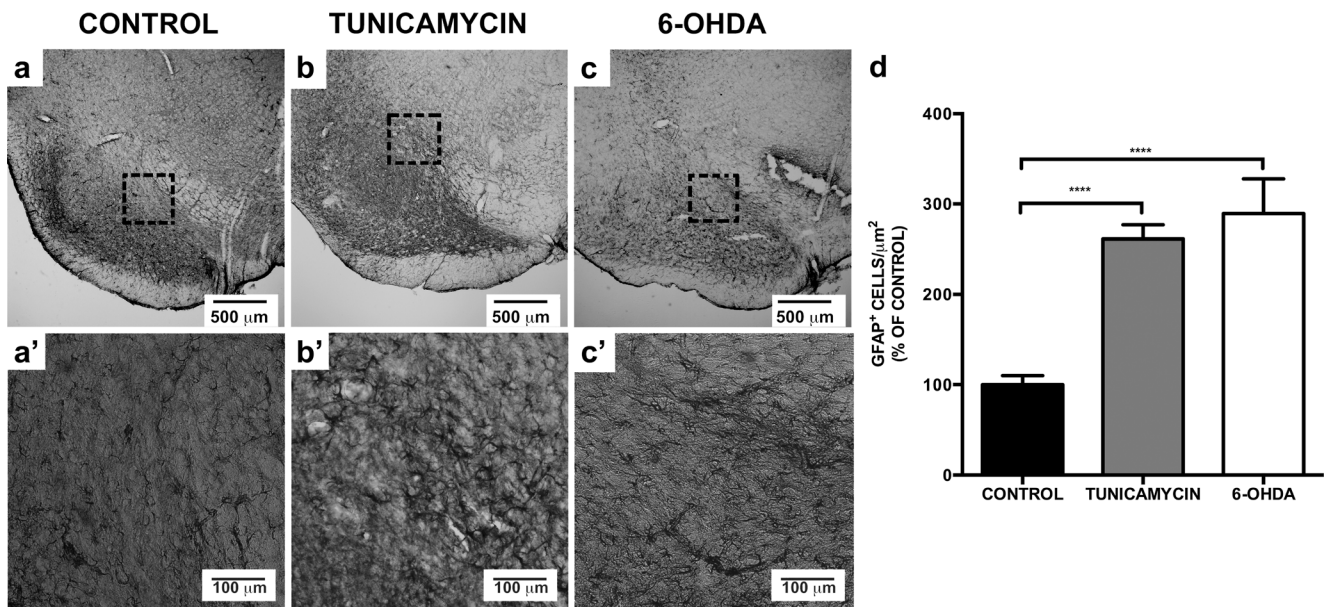
Fig. 3 Reactive astrogliosis in response to Tm lesion. Representative microphotographs showing GFAP-immunoreactivity in SN from **a** Control, **b** Tm and **c** 6-OHDA injected animals 7 days post-lesion. (**a'**–**c'**) Higher magnifications of the boxed areas in **a**–**c**, showing morphology of GFAP-positive cells for Control, Tm and 6-OHDA groups,

respectively. **d** Quantification of GFAP-positive cell number in SNpc. Data are represented as the mean ± SEM (*CONTROL n = 5; TUNICAMYCIN n = 4; 6-OHDA n = 4*). Asterisks indicate statistical differences (****) $p \leq 0.0001$

Fig. 4 Tunicamycin induces α-synuclein oligomerization. **a** Tissue homogenates from SN were immunoblotted against α-synuclein and GAPDH for Control, Tm and 6-OHDA 7 days after treatment. **b** Immunoblot quantification of monomeric α-synuclein and **c** oligomeric α-synuclein. Data are represented as the mean ± SEM (*CONTROL n = 5*; *TUNICAMYCIN n = 4*; *6-OHDA n = 5*). Asterisks indicate statistical differences (***) $p \leq 0.01$
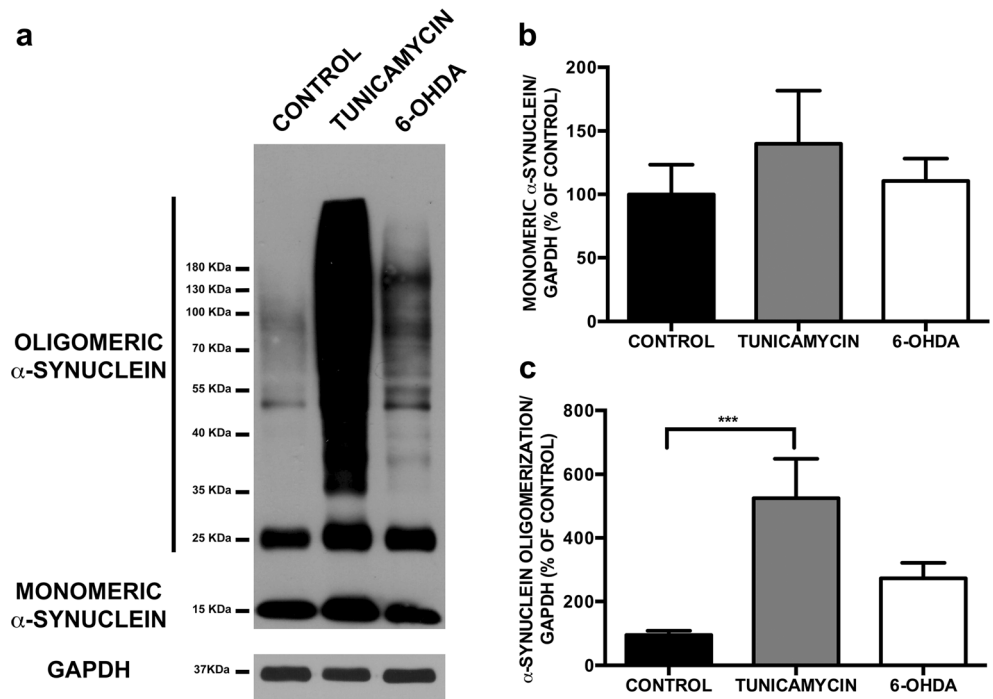

4 (ATF4), CHOP and apoptosis [21, 50]. Different studies demonstrated, in vivo and in vitro, that CHOP-knockout cells are less susceptible to ER stress induced apoptosis [58–60]. This was confirmed later by CHOP knockdown in neuronal cultures that present increased neuronal survival after Tm or thapsigargin exposure [61]. In fact, *chop-/-* mice show protection signs after injection of 6-OHDA in SNpc of adult mice [31], and wild-type mice intracerebroventricularly injected with the same neurotoxin showed an increase in CHOP expression (30). Surprisingly, Tm injected animals did not exhibit increased levels of CHOP when compared to 6-OHDA (Fig. 6), suggesting that neuronal loss induced by Tm injection could be associated to other apoptotic pathways, different from CHOP.

In PD, protein misfolding and aggregation have become one of the central focuses of research. Accumulation of α-synuclein has been linked to progression of neurodegeneration in PD [62, 63], and different studies had related α-synuclein oligomerization with ER-stress condition. Employing an *A53T αS* transgenic mice model, Colla and collaborators showed that symptomatic animals presented increased levels of ER-chaperones and α-synuclein ER accumulation in addition to the α-synuclein oligomers formation and disease progression [45]. Remarkably, in vitro studies

Fig. 5 Tunicamycin and 6-OHDA induce ER-stress in SN. **a** Tissue homogenates from SN were immunoblotted against KDEL (GRP78 and GRP94) and β-actin for control, Tm and 6-OHDA 7 days after treatment. **b–c** Quantification of GRP78 and GRP94 are represented as the mean ± SEM (*CONTROL n = 5*; *TUNICAMYCIN n = 5*; *6-OHDA n = 5*). Asterisks indicate statistical differences (**) $p \leq 0.05$, (***) $p \leq 0.01$
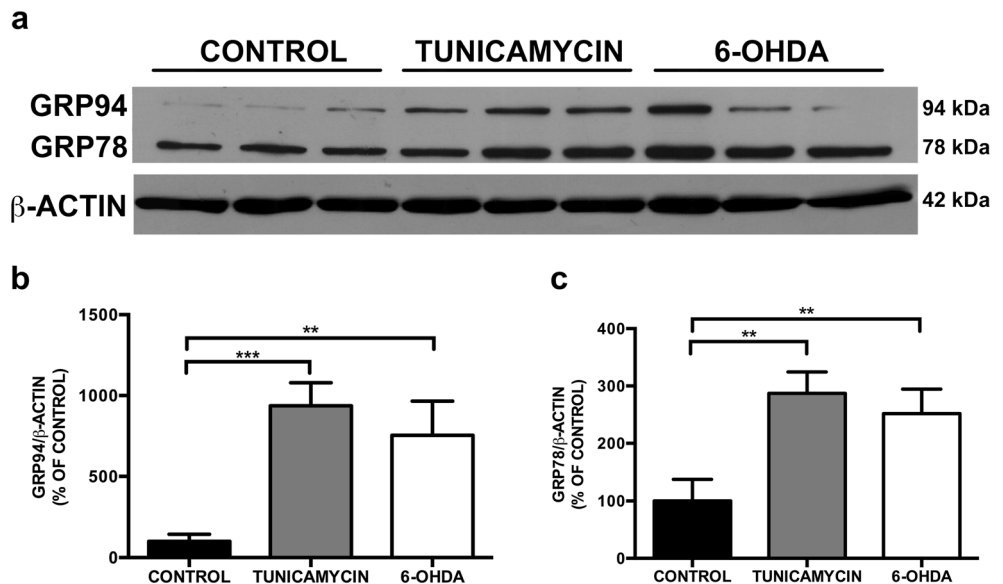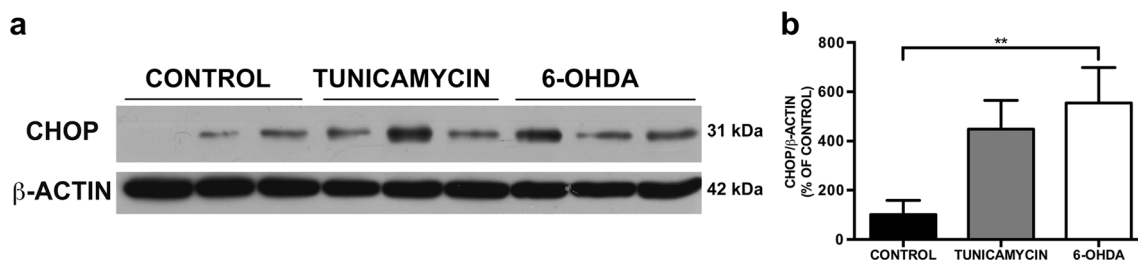
Fig. 6 Activation level of the pro-apoptotic PERK pathway after Tm and 6-OHDA injections. **a** Tissue homogenates from SN were immunoblotted against CHOP and β-actin for protein loading control. **b** Quantification of CHOP is represented as the mean ± SEM (*CONTROL n* = 6; *TUNICAMYCIN n* = 6; *6-OHDA n* = 6), asterisks indicate statistical differences (**) $p \leq 0.05$

showed that increased levels of ER stress induce α-synuclein oligomerization in cells overexpressing wild-type α-synuclein [44, 64]. In the current study, we employed an in vivo pharmacological model of ER stress and showed that the endogenous α-synuclein is extensively oligomerized (Fig. 4a, c) under a Tm challenge. Importantly, animals used in the experiments do not have any genetic manipulation (e.g., α-synuclein transgenic mice), indicating that endogenous levels of α-synuclein are sufficient to produce oligomerized forms of the protein under ER-stress conditions. Interestingly, in accordance with previous results obtained with human neuroblastoma cell line and mice primary neuronal cultures [44, 64], monomeric α-synuclein levels did not change after Tm treatment (Fig. 4a, b), suggesting that oligomerization is not caused by an increased α-synuclein synthesis. In the present study, we observed that Tm treatment was more efficient to produce oligomerized forms of α-synuclein, when compared to 6-OHDA-rat model (Fig. 4a, c). The observed difference in such oligomerization status between Tm- and 6-OHDA-injected animals could be a consequence of the activation of different UPR-associated pathways due to the nature of each ER stressor molecule. However, our results strongly suggest that not only Tm treatment produces α-synuclein oligomers but also 6-OHDA. Unexpectedly, the status of α-synuclein oligomerization has not been previously reported for animals administrated with 6-OHDA, in spite of being a well-established model of Parkinsonism. Further in vivo experiments will be conducted in order to clarify the differences between Tm- and 6-OHDA-induced ER stress and to establish 6-OHDA as a bona fide ER-stressor molecule.

Astrocytes are important players in supporting neurons homeostasis [42, 65]. However, glial reactivity is a major hallmark of every neurodegenerative disease, and because of its relationship with neurons, glial cells could promote the start and progression of neurodegeneration [65–67]. When compared to other CNS regions, SNpc presents the lowest amount of astrocytes [65]. Nevertheless, animal models and post-mortem analyses of patients with PD show increased levels of reactive astroglia in SNpc [68, 69], suggesting that when stressed, these astrocytes could contribute to neurodegenerative progress in PD [65]. In the present study we observed an increase in GFAP+ cell number in SNpc of animals treated with Tm and 6-OHDA, suggesting that ER stress could act as an inducer of astroglial reactivity. Reactive astrogliosis has previously been linked to ER stress induction in mice cortex by a liquid nitrogen lesion model [70], Authors observed that penumbra area was predominantly dominated by reactive GFAP+ cells which express high amounts of BiP and OASIS (Old Astrocyte Specific Induced Substance), two proteins involved with UPR signaling [70].

Tm and 6-OHDA lesions inflicted an increase of stance width for hindpaws (Fig. 1b), suggesting that the occurence of a gait imbalance, since they presented respectively a 25 and 22 % reduction of dopaminergic neurons in SNpc (Fig. 2d). This data are in accordance with previous findings showing that after an intranigral injection of 6-OHDA in an hemiparkinsonian model of PD, footprint tasked animals presented increased distance between hindpaws as soon as 4 days after the lesion [38]. To our knowledge, this is the first demonstration that Tm was employed as an ER-stressor directly in SNpc. It was previously demonstrated that when medaka fish was injected with Tm into cerebrospinal fluid cavity animals presented movement disorder, a behavioral sign related to PD [71]. However, this model presents the limitation of inducing an overall ER-stress, including anatomical regions not directly involved with PD. Furthermore, Fouillet et al. (2012) showed that a chronic intraperitoneal administration of Tm, at low doses, produces a preconditioning with mild UPR that generates neuroprotection in the 6-OHDA mouse model of PD [72]. In contrast, our proposed model employed intranigral drug administration by stereotaxic surgery, which has the advantage to ensure an acute challenge only in a limited region of the CNS and precludes an undesired systemic drug delivery.

Overall, our data confirm that Tm induces in vivo functional and molecular PD conditions, similarly to those induced by 6-OHDA. Induction of UPR and ER stress led to several features of PD, such as α-synuclein oligomerization, dopaminergic neurons death, and locomotor disabilities. Understanding the genesis of PD is necessary for early diagnosis and advances towards the development of new preventive therapies. We believe that future studies employing Tm lesion models and manipulation of UPR pathways will further characterize the role of the ER stress in the development of PD.

References

1. Lang AE, Lozano AM (1998) Parkinson's disease. N Engl J Med 339:1044–1053

2. Shiba M, Bower JH, Maraganore DM, McDonnell SK, Peterson BJ, Ahlskog JE, Schaid DJ, Rocca WA (2000) Anxiety disorders and depressive disorders preceding Parkinson's disease: a case-control study. Mov Disord 15(4):669–677

3. Lima MM, Andersen ML, Reksidler AB, Ferraz AC, Vital MA, Tufik S (2012) Paradoxical sleep deprivation modulates tyrosine hydroxylase expression in the nigrostriatal pathway and attenuates motor deficits induced by dopaminergic depletion. CNS & Neurol Disord Drug Targets 11(4):359–368

4. Dauer W, Przedborski S (2003) Parkinson's disease: mechanisms and models. Neuron 39:889–909

5. Przedborski S (2010) Inflammation and Parkinson's disease pathogenesis. Mov Disord 25(1):S55–S57

6. Tieu K (2011) A guide to neurotoxic animal models of Parkinson's disease. Cold Spring Harb Perspect Med 1(1):a009316. doi:10.1101/cshperspect.a009316

7. Perier C, Vila M (2012) Mitochondrial biology and Parkinson's disease. Cold Spring Harbor perspectives in medicine 2(2):a009332

8. Jellinger KA (2012) Interaction between pathogenic proteins in neurodegenerative disorders. J Cell Mol Med 16(6):1166–1183

9. Dettmer U, Selkoe D, Bartels T (2016) New insights into cellular α-synuclein homeostasis in health and disease. Curr Opin Neurobiol 36:15–22

10. Danzer KM, Haasen D, Karow AR, Moussaud S, Habeck M, Giese A, Kretzschmar H, Hengerer B, Kostka M (2007) Different species of alpha-synuclein oligomers induce calcium influx and seeding. J Neurosci 27(34):9220–9232

11. Hettiarachchi NT, Parker A, Dallas ML, Pennington K, Hung CC, Pearson HA, Boyle JP, Robinson P, Peers C (2009) α-Synuclein modulation of Ca2+ signaling in human neuroblastoma (SH-SY5Y) cells. J. Neurochem 111(5):1192–1201

12. Winklhofer KF, Haass C (2010) Mitochondrial dysfunction in Parkinson's disease. Biochim Biophys Acta 1802(1):29–44

13. Tsang AH, Chung KK (2009) Oxidative and nitrosative stress in Parkinson's disease. Biochim Biophys Acta 1792(7):643–650

14. Chen L, Jin J, Davis J, Zhou Y, Wang Y, Liu J, Lockhart PJ, Zhang J (2007) Oligomeric alpha-synuclein inhibits tubulin polymerization. Biochem Biophys Res Commun 356(3):548–553

15. Qian L, Flood PM, Hong JS (2010) Neuroinflammation is a key player in Parkinson's disease and a prime target for therapy. J Neural Transm 117(8):971–979

16. Spillantini MG, Crowther RA, Jakes R, Hasegawa M, Goedert M (1998) alpha-synuclein in filamentous inclusions of Lewy bodies from Parkinson's disease and dementia with lewy bodies. Proc Natl Acad Sci U S A 95(11):6469–6473

17. Roberts HL, Brown DR (2015) Seeking a mechanism for the toxicity of oligomeric α-synuclein. Biomolecules 5(2):282–305

18. Kim YM, Jang WH, Quezado MM, Oh Y, Chung KC, Junn E, Mouradian MM (2011) Proteasome inhibition induces α-synuclein SUMOylation and aggregate formation. J Neurol Sci 307(1–2):157–161

19. Krumova P, Meulmeester E, Garrido M, Tirard M, Hsiao HH, Bossis G, Urlaub H, Zweckstetter M, Kügler S, Melchior F, Bähr M, Weishaupt JH (2011) Sumoylation inhibits α-synuclein aggregation and toxicity. J Cell Biol 194(1):49–60

20. Martinez-Vicente M, Talloczy Z, Kaushik S, Massey AC, Mazzulli J, Mosharov EV, Hodara R, Fredenburg R, Wu DC, Follenzi A, Dauer W, Przedborski S, Ischiropoulos H, Lansbury PT, Sulzer D, Cuervo AM (2008) Dopamine-modified α-synuclein blocks chaperone-mediated autophagy. J Clin Invest 118(2):777–788

21. Hetz C (2012) The unfolded protein response: controlling cell fate decisions under ER stress and beyond. Nat Rev Mol Cell Biol 13(2):89–102

22. Kim I, Xu W, Reed JC (2008) Cell death and endoplasmic reticulum stress: disease relevance and therapeutic opportunities. Nat Rev Drug Discov 7(12):1013–1030

23. Boyce M, Yuan J (2006) Cellular response to endoplasmic reticulum stress: a matter of life or death. Cell Death Differ 13(3):363–373

24. Yoshida H (2007) ER stress and diseases. FEBS J 274(3):630–658

25. Hoozemans JJM, Scheper W (2012) Endoplasmic reticulum: the unfolded protein response is tangled in neurodegeneration. Int J Biochem Cell Biol 44(8):1295–1298

26. Hetz C, Mollereau B (2014) Disturbance of endoplasmic reticulum proteostasis in neurodegenerative diseases. Nat Rev Neurosci 15(4):233–249

27. Mercado G, Castillo V, Soto P, Sidhu A (2016) ER stress and Parkinson's disease: pathological inputs that converge into the secretory pathway. Brain Res. doi:10.1016/j.brainres.2016.04.042

28. Hoozemans JJM, Van Haastert ES, Eikelenboom P, Vos D, R. al, Rozemuller JM, Scheper W (2007) Activation of the unfolded protein response in Parkinson's disease. Biochem Biophys Res Commun 354(3):707–711

29. Holtz WA, O'Malley KL (2003) Parkinsonian mimetics induce aspects of unfolded protein response in death of dopaminergic neurons. J Biol Chem 278(21):19367–19377

30. Tanaka K, Fukuoka S, Kawahara S, Kimoto N, Ogawa N (2013) Effect of cabergoline on increase of several ER stress-related molecules in 6-OHDA-lesioned mice. Neurol Sci 34(2):259–261

31. Silva RM, Ries V, Oo TF, Yarygina O, Jackson- V, Ryu EJ, Lu PD, Marciniak SJ, Ron D, Przedborski S, Kholodilov N, Greene LA, Burke RE (2005) CHOP/GADD153 is a mediator of apoptotic death in substantia nigra dopamine neurons in an in vivo neurotoxin model of parkinsonism. J Neurochem 95(4):974–986

32. Ryu EJ, Harding HP, Angelastro JM, Vitolo OV, Ron D, Greene LA (2002) Endoplasmic reticulum stress and the unfolded protein response in cellular models of Parkinson's disease. J Neurosci 22(24):10690–10698

33. Credle JJ, Forcelli PA, Delannoy M, Oaks AW, Permaul E, Berry DL, Duka V, Wills J, Sidhu A (2015) Alpha-synuclein-mediated inhibition of ATF6 processing into COPII vesicles disrupts UPR signaling in Parkinson's disease. NeurobiolDis 76:112–125

34. Egawa N, Yamamoto K, Inoue H, Hikawa R, Nishi K, Mori K, Takahashi R (2011) The endoplasmic reticulum stress sensor, ATF6alpha, protects against neurotoxin-induced dopaminergic neuronal death. J Biol Chem 286(10):7947–7957

35. Valdés P, Mercado G, Vidal RL, Molina C, Parsons G, Court FA, Martinez A, Galleguillos D, Armentano D, Schneider BL, Hetz C (2014) Control of dopaminergic neuron survival by the unfolded protein response transcription factor XBP1. Proc Natl Acad Sci U S A 111(18):6804–6809

36. Leaver DD, Schneider KM, Rand MJ, Anderson RM, Gage PW, Malbon R (1988) The neurotoxicity of tunicamycin. Toxicology 49:179–187

37. Ebert DA, Hann HJ, Bohn MC (2008) Progressive degeneration of dopamine neurons in 6-hydroxydopamine rat model of Parkinson's

disease does not involve activation of caspase-9 and caspase-3. J Neurosci Res 86:317–325

38. Hsieh T-H, Chen J-JJ, Chen L-H, Chiang P-T, Lee H-Y (2011) Time-course gait analysis of hemiparkinsonian rats following 6-hydroxydopamine lesion. Behav Brain Res 222(1):1–9

39. Carter, R. J., Morton J., Dunnet, S. B. (2001). Motor coordination and balance in rodents. Curr Protoc Neurosci, Chapter 8: Unit 8.12. doi: 10.1002/0471142301.ns0812s15

40. Pallier PN, Drew CJG, Morton AJ (2009) The detection and measurement of locomotor deficits in a transgenic mouse model of Huntington's disease are task- and protocol-dependent: influence of non-motor factors on locomotor function. Brain Res Bull 78(6):347–355

41. Carter RJ, Lione LA, Humby T, Mangiarini L, Mahal A, Bates GP, Dunnett SB, et al. (1999) Characterization of progressive motor deficits in mice transgenic for the human Huntington' s disease mutation. J Neurosci 19(8):3248–3257

42. Sofroniew MV, Vinters HV (2010) Astrocytes: biology and pathology. Acta Neuropathol 119(1):7–35

43. Kikuchi H, Almer G, Yamashita S, Guégan C, Nagai M, Xu Z, Sosunov A a, et al. (2006) Spinal cord endoplasmic reticulum stress associated with a microsomal accumulation of mutant superoxide dismutase-1 in an ALS model. Proc Natl Acad Sci U S A 103(15): 6025–6030

44. Jiang P, Gan M, Ebrahim AS, Lin W-L, Melrose HL, Yen S-HC (2010) ER stress response plays an important role in aggregation of α-synuclein. Mol Neurodegener 5(1):56. doi:10.1186/1750-1326-5-56

45. Colla E, Coune P, Liu Y, Pletnikova O, Troncoso JC, Iwatsubo T, Schneider BL, et al. (2012) Endoplasmic reticulum stress is important for the manifestations of α-synucleinopathy in vivo. J Neurosci 32(10):3306–3320

46. Dawson TM, Dawson VL (2003) Molecular pathways of neurodegeneration in Parkinson's disease. Science 302:819–822

47. Mori K (2000) Tripartite management of unfolded Proteins in the endoplasmic reticulum. Cell 101:451–454

48. Ron D, Walter P (2007) Signal integration in the endoplasmic reticulum unfolded protein response. Nat Rev Mol Cell Biol 8:519–529

49. Gardner BM, Pincus D, Gotthardt K, Gallagher CM, Walter P (2013) Endoplasmic reticulum stress sensing in the unfolded protein response. Cold Spring Harb Perspect Biol 5(3):a013169

50. Tabas I, Ron D (2011) Integrating the mechanisms of apoptosis induced by endoplasmic reticulum stress. Nat Cell Biol 13(3): 184–190

51. Hoozemans JJM, Van Haastert ES, Nijholt D a T, Rozemuller AJM, Scheper W (2012) Activation of the unfolded protein response is an early event in Alzheimer's and Parkinson's disease. Neurodegener Dis 10(1–4):212–215

52. Bové J, Prou D, Perier C, Przedborski S (2005) Toxin-induced models of Parkinson's disease. NeuroRx 2(3):484–494

53. Liu ZC, Fu ZQ, Song J, Zhang JY, Wei YP, Chu J, Han L, Qu N, Wang JZ, Tian Q (2012) Bip enhanced the association of GSK-3b with tau during ER stress both in vivo and in vitro. J Alzheimers Disease 29(4):727–740

54. Okada T, Yoshida H, Akazawa R, Negishi M, Mori K (2002) Distinct roles of activating transcription factor 6 (ATF6) and double-stranded RNA-activated protein kinase-like endoplasmic reticulum kinase (PERK) in transcription during the mammalian unfolded protein response. Biochem J 366:585–594

55. Oyadomari S, Mori M (2004) Roles of CHOP/GADD153 in endoplasmic reticulum stress. Cell Death Differ 11(4):381–389

56. Rutkowski DT, Kaufman RJ (2004) A trip to the ER: coping with stress. Trends Cell Biol 14(1):20–28

57. Lu W, Hagiwara D, Morishita Y, Tochiya M, Azuma Y, Suga H, Goto M, Banno R, Sugimura Y, Oyadomari S, Mori K, Arima H (2016) Unfolded protein response in hypothalamic cultures of wild-type and ATF6α-knockout mice. Neurosci Lett 612:199–203

58. Rutkowski DT, Arnold SM, Miller CN, Wu J, Li J, Gunnison KM, Mori K, et al. (2006) Adaptation to ER stress is mediated by differential stabilities of pro-survival and pro-apoptotic mRNAs and proteins. PLoS Biol 4(11):e374

59. Zinszner H, Kuroda M, Wang X, Batchvarova N, Lightfoot RT, Remotti H, Stevens JL, Ron D (1998) CHOP is implicated in programmed cell death in response to impaired function of the endoplasmic reticulum. Genes Dev 12:982–995

60. Marciniak SJ, Yun CY, Oyadomari S, Novoa I, Zhang Y, Jungreis R, Nagata K, et al. (2004) CHOP induces death by promoting protein synthesis and oxidation in the stressed endoplasmic reticulum. Genes Dev 18(24):3066–3077

61. Galehdar Z, Swan P, Fuerth B, Callaghan SM, Park DS, Cregan SP (2010) Neuronal apoptosis induced by endoplasmic reticulum stress is regulated by ATF4-CHOP-mediated induction of Bcl-2 homology 3-only member PUMA. J Neurosci 30(50):16938–16948

62. Zhang W, Wang T, Pei Z, Miller DS, Wu X, Block ML, Wilson B, Zhang W, Zhou Y, Hong JS, Zhang J (2005) Aggregated α-synuclein activates microglia: a process leading to disease progression in Parkinson's disease. FASEB J 19(6):533–542

63. Winner B, Jappelli R, Maji S, K. D, P. A, Boyer L, Aigner S, Hetzer C, Loher T, Vilar M, Campioni S, Tzitzilonis C, Soragni A, Jessberger S, Mira H, Consiglio A, Pham E, Masliah E, Gage FH, Riek R (2011) In vivo demonstration that α-syniclein oligomers are toxic. Proc Natl Acad Sci U S A 108(10):4194–4199

64. Jiang P, Gan M, Lin W-L, Yen S-HC (2014) Nutrient deprivation induces α-synuclein aggregation through endoplasmic reticulum stress response and SREBP2 pathway. Front Aging Neurosci 6: 268. doi:10.3389/fnagi.2014.00268

65. Heneka MT, Rodríguez JJ, Verkhratsky A (2010) Neuroglia in neurodegeneration. Brain Res Rev 63(1–2):189–211

66. Papadeas ST, Kraig SE, O'Banion C, Lepore AC, Maragakis NJ (2011) Astrocytes carrying the superoxide dismutase 1 (SOD1G93A) mutation induce wild-type motor neuron degeneration in vivo. Proc Natl Acad Sci U S A 108(43):17803–17808

67. Díaz-Amarilla P, Olivera-Bravo S, Trias E, Cragnolini A, Martínez-Palma L, Cassina P, Beckman J, Barbeito L (2011) Phenotypically aberrant astrocytes that promote motoneuron damage in a model of inherited amyotrophic lateral sclerosis. Proc Natl Acad Sci U S A 108(44):18126–18131

68. Langston JW, Forno LS, Tetrud J, Reeves AG, Kaplan JA, Karluk D (1999) Evidence of active nerve cell degeneration in the substantia nigra of humans years after 1-methyl-4-phenyl-1,2,3,6-tetrahydropyridine exposure. Ann Neurol 46(4):598–605

69. Damier P, Hirsch CE, Zhang P, Agid Y, Javoy-Agid F (1993) Glutathione peroxidase, glial cells and Parkinson's disease. Neuroscience 52(1):1–6

70. Kondo S, Murakami T, Tatsumi K, Ogata M, Kanemoto S, Otori K, Iseki K, et al. (2005) OASIS, a CREB/ATF-family member, modulates UPR signalling in astrocytes. Nat Cell Biol 7(2):186–194

71. Matsui H, Ito H, Taniguchi Y, Takeda S, Takahashi R (2010) Ammonium chloride and tunicamycin are novel toxins for dopaminergic neurons and induce Parkinson's disease-like phenotypes in medaka fish. J Neurochem 115(5):1150–1160

72. Fouillet A, Levet C, Virgone A, Robin M, Dourlen P, Rieusset J, Belaidi E, Ovize M, Touret M, Nataf S, Mollereau B (2012) ER stress inhibits neuronal death by promoting autophagy. Autophagy 8(6):915–926